

LONG BASELINE ACCELERATOR NEUTRINO EXPERIMENTS: PRESENT AND FUTURE*

ANDRÉ RUBBIA

Institut für Teilchenphysik, ETHZ
CH-8093 Zürich, Switzerland

(Received May 10, 2000)

A ν_μ disappearance effect has been seen in atmospheric neutrino experiments. This has led to the “evidence for neutrino oscillations”. The next problem in neutrino physics is to perform the right experiment(s) to *elucidate in a comprehensive way the pattern of neutrino masses and mixings*. The long baseline experiments will play a fundamental role at settling definitively the question of flavor oscillation and at measuring with good precision the oscillation parameters. The CERN–NGS beam coupled with the proposed ICANOE and OPERA detectors is the only programme capable of sensitive tau and electron appearance searches.

PACS numbers: 14.60.Pq, 14.60.Lm

1. Introduction

The “atmospheric neutrino anomaly”, first published by Kamiokande in 1988 [1] and, at the time, quite controversial, has been strongly confirmed by the latest measurements from SuperKamiokande [2], Soudan-II [3] and MACRO [4]. The results of the atmospheric neutrino experiments stand today as strong evidence that muon neutrinos are “disappearing”.

The most logical and attractive way to explain these results is by invoking neutrino flavor oscillations. In particular, SuperKamiokande has dubbed this observation as a clear “evidence for neutrino oscillations” [2]. Under this hypothesis, the probability for a flavor oscillation will be given by $P = \sin^2 2\theta \sin^2(1.27\Delta m^2 L/E)$ where θ is a mixing angle, Δm^2 is the difference of the squared masses (in eV^2), L is the path-length (in km) and E is the neutrino energy (in GeV).

* Presented at the Cracow Epiphany Conference on Neutrinos in Physics and Astrophysics, Cracow, Poland, January 6–9, 2000.

2. What is the mixing matrix?

At first, it came with some surprise that the mixing angle involved in the disappearance of the atmospheric neutrino is so large, in fact, compatible with being maximal. Under the hypothesis that $\nu_\mu \rightarrow \nu_\tau$ oscillations take place, this would indicate that the muon and the tau neutrinos are fully mixed with respect to their mass eigenstates. The electron data indicates that the electron neutrino does not participate in the observed phenomenon.

If we consider in general that the mixing should be described by a 3×3 matrix involving all three neutrino flavors, the oscillation pattern may be complicated and introduce a combination of transitions to ν_e, ν_μ, ν_τ . By symmetry with the quark sector, it is in addition natural to expect CP violation at some level.

Clearly, the first main question that remains unanswered is whether the disappearance of ν_μ atmospheric neutrinos is due to neutrino “flavor” oscillation, *i.e.* to the “appearance” of the ν_τ flavor. At present, it is not possible to answer this question with certainty. But a second urgent question is determination of the full mixing matrix, including possible oscillations involving the first generation, *i.e.* $\nu_\mu \rightarrow \nu_e$ transitions at the atmospheric Δm^2 .

The test of the oscillation phenomenon in the region of Δm^2 indicated by atmospheric neutrinos requires experiments at long baselines (LBL) with capabilities of disappearance and appearances of electron and tau flavors.

3. Planned LBL programs

There are three long baseline programs: one in Japan (K2K), one in America (NUMI [5]) and one in Europe (CNGS [6]). Early results from K2K have been reported by Kielczewska [7]. Para reported on the oscillation program at FNAL [5]. The main parameters of NUMI and CNGS are shown in Table I and compared to the CERN-WANF¹. These beams require multikton detectors in order to collect sufficient events. From the table, it is clear that the NGS beam is built on the extensive past experience acquired at CERN.

High energy implies that $E_{\text{cm}} \gg m_\tau$, in order to efficiently produce via charged current the tau lepton in case of appearance of ν_τ neutrinos. The CERN-NGS and FNAL-NUMI beams are both very appealing for direct $\nu_\mu \rightarrow \nu_\tau$ appearance experiments. To achieve a clear tau appearance signal over small backgrounds imposes however constraints on the detector design, in particular on their granularity.

¹ The CERN-WANF symbolizes the CERN experience in neutrino beams, acquired over more than 20 years of operation.

TABLE I

List of relevant parameters for the present CERN neutrino beam and for the anticipated beams at KEK, at Fermilab and at CERN.

	CERN-WANF	FNAL-NUMI	CERN-NGS
<i>Protons:</i>			
Energy (GeV)	450	120	400
Pot/cycle	2×10^{13}	4×10^{13}	$4 \times 2.3 \times 10^{13}$
Cycle time (s)	14.4	1.9	26.4
Days/year	200×0.75	300×0.67	200×0.75
Pot/year	1.5×10^{19}	3.7×10^{20}	4.5×10^{19}
<i>Long-baseline ν's:</i>			
$\langle E(\nu_{\mu}CC) \rangle$	—	3-16 GeV	17 GeV
ν_{μ} CC/kt/ 10^{19}	—	13-86	545
ν_{μ} CC/year	—	460 – 3200/kt	2450/kt
ν_{τ} appearance	—	Yes/No	Yes
<i>Status:</i>			
Running date	→ 1998	2003 →	2005 →

FNAL-NUMI beam has three options: PH2(low), PH2(medium), PH2(high). The CERN-NGS figures correspond to a “shared” mode of operation.

The general strategy at the CNGS was to opt for a wide band neutrino beam based on the experience gathered at CERN with the design and the operation of the WANF. The beam optimization and the design of the details of the beam optics have been subject of further studies driven by the requests of the experiments. Following the indication of the CERN-LNGS committee, a first optimization of the beam has been carried out with the goal of maximizing the ν_{τ} CC interactions at LNGS for appearance experiments.

The expected event rates without oscillations per kton and year in shared mode are 2450 ν_{μ} CC, 49 $\bar{\nu}_{\mu}$ CC, 20 ν_e CC, 1.2 $\bar{\nu}_e$ CC, 823 ν NC, and 17 $\bar{\nu}$ NC. The rates for tau appearance in shared running mode are 2.4 events/kton/year for $\Delta m^2 = 1 \times 10^{-3}$ eV², 29.4 events/kton/year for 3.5×10^{-3} eV² and 58.6 events/kton/year for 5×10^{-3} eV².

4. Overview LBL detectors

There are various types of detector optimizations that can be performed depending on the type of measurement to be achieved:

- **Disappearance:** observed over expected CC ratio. This requires the help of a “near” detector.

- **Appearance:** from an anomalous “NC”/CC ratio. This requires an ability to discriminate between NC and CC events. Neutral current usually englobes all events without a leading muon.
- **Direct appearance:** to pinpoint the oscillation channels. For $\nu_\mu \rightarrow \nu_e$, this requires excellent electron identification, good π^0 rejection, *i.e.* a good granularity. For $\nu_\mu \rightarrow \nu_\tau$, this requires a new generation of τ detectors with large mass and tau lepton identification capabilities.

There have been numerous proposals at the CERN-NGS. Today, two projects, the ICANOE and OPERA detectors, stand as serious options. They are together with the MINOS detector listed in Table II.

TABLE II

List of LBL experiments and sensitivity to $\nu_\mu \rightarrow \nu_\tau$ oscillations

	MINOS	ICANOE	OPERA
<i>Instrumented mass:</i>	5.4 kt	9 kt	1.5 kt
<i>Technology:</i>	Fe+B-Field + scintillator	LAr imaging TPC + fine grain cal +magn. spectrometer	Pb target + emulsion
<i>Main sensitivity:</i>	ν_μ disapp.	ν_e, ν_τ appearance atmospheric ν 's	ν_τ appearance
<i>Tau appearance (4 years “shared” running CNGS):</i>			
Fully identified tau events:			
$2 \times 10^{-3} \text{ eV}^2$		12	4.6
$3 \times 10^{-3} \text{ eV}^2$		26	10.5
$3.5 \times 10^{-3} \text{ eV}^2$		35	14.3
$5 \times 10^{-3} \text{ eV}^2$		71	29
$7 \times 10^{-3} \text{ eV}^2$		121	57
$10 \times 10^{-3} \text{ eV}^2$		248	117
Background		5.1	0.43

For ICANOE, only electron channel for tau appearance is included. For OPERA, five Supermodules (3 spacer + 2 compact) were assumed.

In order to fully sort out the mixing matrix, unambiguous neutrino flavor identification is mandatory to distinguish τ 's from ν_τ 's and electrons from ν_e 's interactions. The CERN-NGS beam coupled with the proposed ICANOE [8–11] and OPERA [12] detector is the only programme capable of sensitive tau and electron appearance searches.

We stress the importance of constraining the oscillation scenarios by coupling appearance in several different channels and disappearance signatures.

4.1. Detection of τ from ν_τ CC interactions

Based on the NOMAD and CHORUS expertise developed at CERN, detectors capable of detecting the presence of tau lepton in the event final states have been proposed. Two different tools are used to reject backgrounds:

- **kinematical selection:** this requires good particle identification and resolution in momentum imbalance (unseen ν 's).
- **direct observation of the decay topology “signature”:** The $\gamma c\tau \approx 0.5 - 1$ mm requires emulsions with μm 's granularity.

The ICANOE (kinematical selection) and OPERA (decay topology) detectors have the potentiality to unambiguously prove the flavor oscillation. The number of fully reconstructed and identified tau events after 4 years of running in shared mode (1.8×10^{20} pots) is shown in Table II. These rates compared to the low levels of backgrounds are sufficient to cover completely the Δm^2 region indicated by the SuperKamiokande results.

5. ICANOE

The ICANOE layout (figure 1) is similar to that of a “classical” neutrino detector, segmented into almost independent **Supermodules**. The layout of the apparatus can be summarized as follows:

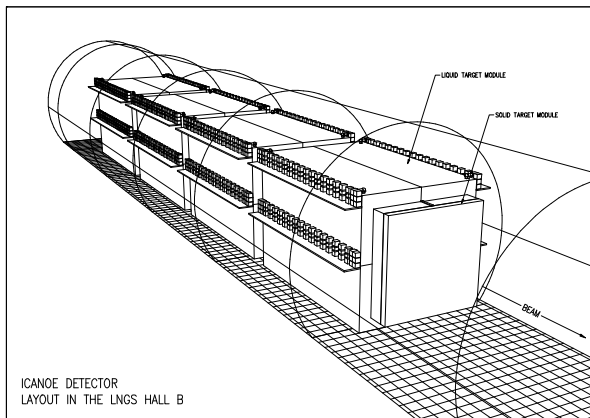


Fig. 1. ICANOE detector in Hall B of LNGS

- the **liquid target**, with extremely high granularity (see figure 2 [13]), dedicated to tracking, dE/dx measurements, full e.m. calorimetry and hadronic calorimetry, where electrons and photons are identified and measured with extremely good precision and π/μ , K and p separation is possible at low momenta;

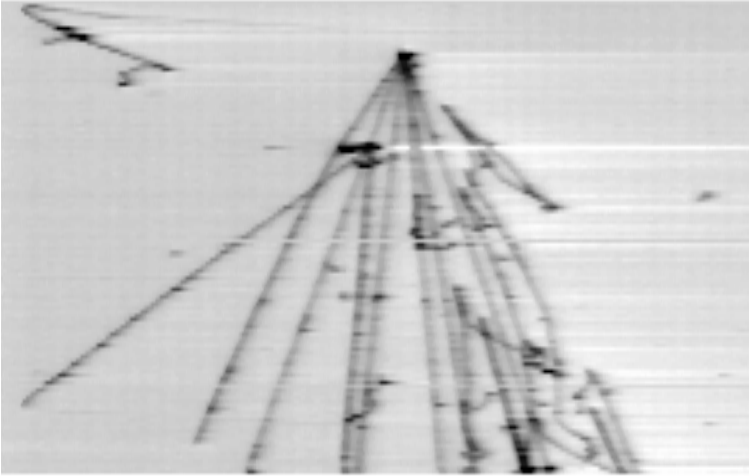


Fig. 2. An example of recorded neutrino interaction in a 50 liter Liquid Argon TPC prototype exposed at the CERN ν beam. The neutrino comes from the top of the picture. The horizontal axis is the time axis (drift direction) and vertically is the wire number. The visible area corresponds to $47 \times 32 \text{ cm}^2$

- the **solid target**, with good e.m. and hadronic resolution, dedicated to calorimetry of the jet and a magnetic field for measurement of the muon features (sign and momentum).

The **Supermodule**, obtained joining a liquid and solid module, which constitutes the basic module of an *expandable* apparatus. A Supermodule behaves as a complete building block, capable of identifying and measuring electrons, photons, muons and hadrons produced in the events. The solid, high density sector reduces the transverse and longitudinal size of hadron shower, confining the event (apart from the muon) within the Supermodule.

At this stage, *four* Supermodules with a total length of the experiment of 82.5 m and a total active mass of 9.3 kton fully instrumented are being considered for the baseline option.

5.1. Physics goals

ICANOE is an underground detector capable to achieve the full reconstruction of neutrino (and antineutrino) events of *any* flavor, and with an energy ranging from the tens of MeV to the tens of GeV, for the relevant physics analyses. No other combinations can provide such a rich spectrum of physical observations. The unique lepton capabilities of ICANOE are really fundamental in tagging the neutrino flavor.

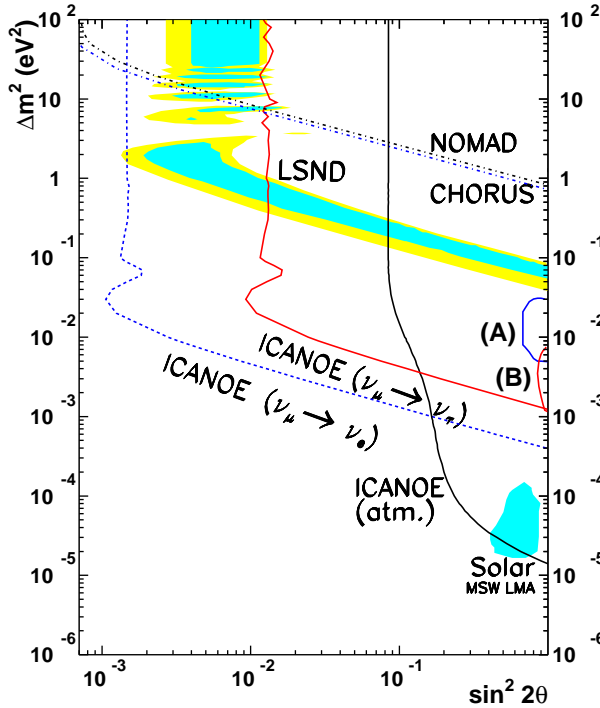


Fig. 3. Overview of the status of the neutrino oscillations searches, displayed assuming two neutrino mixing schemes in the $(\sin^2 2\theta, \Delta m^2)$ plane. The 90% C.L. allowed regions obtained from the Kamiokande (resp. SuperKamiokande) FC and PC samples are shown as (A) (resp. (B)). The 90% (resp. 99% C.L.) regions consistent with the LSND excess are shown as dark (resp. light) shaded areas in the upper region of the plane. The shaded area in the region $\Delta m^2 \approx 10^{-5} \text{ eV}^2$ represents the large angle MSW solution of the solar neutrino deficit. CHORUS and NOMAD 90% C.L. limits on $\nu_\mu \rightarrow \nu_\tau$ oscillations are visible in the upper Δm^2 region. The ICANOE sensitivities at 90% C.L. are indicated by three curves: the limit by direct observation of the atmospheric neutrinos (“ICANOE atm”); the direct tau appearance search at the CNGS (“ICANOE $\nu_\mu \rightarrow \nu_\tau$ ”); the direct electron appearance search at the CNGS (“ICANOE $\nu_\mu \rightarrow \nu_e$ ”).

The sensitivity in the classic $(\sin^2 2\theta, \Delta m^2)$ plot is evidenced in figure 3, for a data taking time of 4 years, with 4.5×10^{19} pot at each year. We remark:

1. The recent results on atmospheric neutrinos ((A) and (B) of figure 3) can be thoroughly explored by appearance and disappearance experiments. For the current central value, both CNGS and cosmic ray data will give independent and complementary measurements and they will provide a precise $(\sin^2 2\theta, \Delta m^2)$ determination.
2. In the mass range of LSND, the sensitivity is sufficient in order to solve definitely the puzzle.
3. At high masses of cosmological relevance for $\Delta m^2 \lesssim 10 \text{ eV}^2$, the sensitivity to $\nu_\mu \rightarrow \nu_\tau$ oscillations is better or equal to the one of CHORUS and NOMAD.
4. In the atmospheric neutrino events, one can reach a level of sensitivity sufficient to detect also the effect until now observed in solar neutrinos. This purely terrestrial detection of the LMA solar neutrino solution is performed using neutrino in the GeV range, much higher than the one of solar neutrinos.

Since we can observe and unambiguously identify both ν_e and ν_τ components, the full (3×3) mixing matrix can be explored. By itself, this is one of the main justifications for the choice of the detector's mass.

In the cosmic ray channel, all specific modes (electron, muon, NC) are equally well observed without detector biases and down to kinematical threshold. The CR-spectrum being rather poorly known, a confirmation of the SuperKamiokande result requires detecting both (1) the modulation in the muon channel and (2) the lack of effect of the electron channel. The consistency of the simultaneous observation of the L/E phenomenon, in as many modes as they are available, is a powerful tool in separating genuine flavour oscillations from exotic scenarios.

In some favourable conditions, the direct appearance of the oscillated tau neutrino may be directly identified in the upgoing events, since even a few events will be highly significant.

For a discussion on the nucleon decay searches, see Ref. [14].

5.2. Physics at the CNGS

As reference for CNGS studies, we assume an exposure of $20 \text{ kton} \times \text{year}$ for the liquid argon. This corresponds to four years running of the CNGS beam in shared mode. For the events occurring in the solid detector, given

the smaller mass, the reference exposure is $10 \text{ kton} \times \text{year}$. The last three meters of the liquid target are defined as a transition region, since beam events occurring in this region are most likely to deposit energy in both targets.

Table III shows the computed total event rates for each neutrino species present in the beam for the liquid, solid and in the transition region. Table III also shows, for three different values of Δm^2 , the ν_τ CC rates expected in case oscillations take place.

TABLE III

Expected event rates for an exposure of $20 \text{ kton} \times \text{year}$ for the liquid target and $10 \text{ kton} \times \text{year}$ for the solid target. All the rates include nuclear corrections and are computed for the proper target composition. For standard processes, no oscillations is assumed. For ν_τ CC, we take two neutrino $\nu_\mu \rightarrow \nu_\tau$ with $\sin^2 2\theta = 1$.

Process	liquid target	transition	solid
ν_μ CC	54300	10200	27150
$\bar{\nu}_\mu$ CC	1090	200	545
ν_e CC	437	80	219
$\bar{\nu}_e$ CC	29	5	15
ν NC	17750	3330	8875
$\bar{\nu}$ NC	410	77	205
ν_τ CC, Δm^2 (eV ²)			
1×10^{-3}	52	10	26
2×10^{-3}	208	40	104
3.5×10^{-3}	620	115	310
5×10^{-3}	1250	235	625
7.5×10^{-3}	2850	535	1425
1×10^{-2}	4330	810	2165

5.3. Event kinematics and tau identification

Kinematical identification of the τ decay, which follows the ν_τ CC interaction requires excellent detector performance: good calorimetric features together with tracking and event topology reconstruction capabilities. The background from standard processes are, depending on the decay mode of the tau lepton considered, the ν_e CC events and/or the ν_μ CC and ν NC events.

In order to separate separate ν_τ events from the background, two basic criteria, already adopted by the short baseline NOMAD experiment, can be used:

- an unbalanced total transverse momentum due to neutrinos produced in the τ decay,
- a kinematical isolation of hadronic prongs and missing momentum in the transverse plane.

In addition, given the baseline L between CERN and GranSasso, for the lower Δm^2 values of the allowed region indicated by the atmospheric neutrino results, we expect most of the oscillation to occur at low energy. In this case, a criteria on the visible energy is also very important to suppress backgrounds.

In order to apply the most efficient kinematic selection, it is mandatory to reconstruct with the best possible resolution the energy and the angle of the hadronic jet, with a particular attention to the tails of the distributions. Therefore, the energy flow algorithm should be designed with care taking into account the needs of the tau search analyses.

A specially developed energy flow algorithm has been tested on a sample of fully simulated ν_e CC events, in order to estimate the resolution of the kinematical reconstruction on realistic events. It yields an average missing P_T of 450 MeV/ c . This value improves to an average of 410 MeV/ c when the primary vertex is required to lie within a fiducial volume of transverse dimensions $7.8 \times 7.8\text{m}^2$.

We used the neutrino data collected in the NOMAD detector to probe the reliability of the physics simulation. ν_μ CC events have been fully simulated and reconstructed using NOMAD official packages. We found that the kinematics in the transverse plane are well reproduced by the Monte-Carlo model. This is clearly not the case when nuclear corrections are neglected.

TABLE IV

Rejection of the ν_e CC background in the $\tau \rightarrow e$ analysis. Figures are normalized to an exposure of 20 kton \times year.

Cuts	ν_τ Eff. (%)	ν_e CC	$\bar{\nu}_e$ CC	ν_τ CC $\Delta m^2 =$ 10^{-3} eV^2	ν_τ CC $\Delta m^2 =$ $3.5 \times 10^{-3} \text{ eV}^2$	ν_τ CC $\Delta m^2 =$ 10^{-2} eV^2
Initial	100	437	29	9.3	111	779
Fiducial volume	88	383	25	8.2	97	686
One candidate with momentum > 1 GeV	72	365	25	6.7	80	561
$E_{\text{vis}} < 18$ GeV	67	64	5	6.2	75	522
$P_T^{\tau} < 0.9$ GeV	54	31	3	5.0	60	421
$P_T^{\text{lep}} > 0.3$ GeV	51	29	2	4.7	56	397
$P_T^{\text{miss}} > 0.6$ GeV	33	4	0.4	3.1	37	257

5.4. $\nu_\mu \rightarrow \nu_\tau$ appearance searches

The channel of tau decaying into an electron plus two neutrinos provides the best sample for ν_τ appearance studies due to the low background level. The intrinsic $\nu_e, \bar{\nu}_e$ contaminations of the beam amount to ≈ 470 events for an exposure of 20 kton \times year.

The comparison of this figure with the expected number of ν_τ CC events decaying into electrons shows that the search of $\tau \rightarrow e$ at the CNGS will have to be optimized *a posteriori*. Indeed the ν_τ rate has a strong dependence on the exact value of the Δm^2 in the parameter region suggested by the SuperKamiokande data, and the Δm^2 value is not well constrained by the atmospheric neutrino experiments.

For “large” values of Δm^2 , *i.e.* $\Delta m^2 > 5 \times 10^{-3}$, the rate of tau is spectacular and exceeds the number of intrinsic beam $\nu_e, \bar{\nu}_e$ CC events, *i.e.* $S/B > 1$ even prior to any kinematical cuts. So the kinematical cuts can be very mild. An excess will be striking.

For our “best” value taken from atmospheric neutrino results, *i.e.* $\Delta m^2 = 3.5 \times 10^{-3}$ eV², the number of ν_τ CC with $\tau \rightarrow e$ is about 110, or about a signal over background ratio of 110/470 $\simeq 1/4$. Here with modest kinematical cuts, we can extract statistically significant signals, as shown in the following sections.

The most difficult region lies below $\Delta m^2 \approx 1.5 \times 10^{-3}$ eV², for which, kinematical cuts are tuned to suppress backgrounds by a factor more than 200 while keeping about half of the signal events.

TABLE V

ν_μ NC background to the $\tau \rightarrow e$ analysis. Results are normalized to an exposure of 20 kton \times year. We illustrate background reduction by means of kinematical criteria only. Imaging and dE/dx measurements reduce the NC background to a negligible level.

Cuts	ν_μ NC			
Initial	17750			
Fiducial volume	15550			
	Dalitz	γ conv.	$\pi \rightarrow e$	π^\pm/π^0
One candidate	275	4262	6.5	25
$P_e > 1$ GeV	79	1361	6.3	16
$E_{\text{vis}} < 18$ GeV	49	835	3.2	11
$P_T^e < 0.9$ GeV	46	794	1.8	9
$P_T^{\text{lep}} > 0.3$ GeV	24	429	1.7	8
$P_T^{\text{miss}} > 0.6$ GeV	19	350	1.3	7
Imaging and dE/dx	< 1	< 1	< 1	< 1

In the following paragraphs, we discuss background sources and their suppression.

ν_e CC rejection: The main background from genuine leading electrons comes from the CC interactions of the ν_e and $\bar{\nu}_e$ components of the beam. In Table IV we summarize the list of sequential cuts applied to reduce the ν_e and $\bar{\nu}_e$ CC backgrounds and the expected number of signal events for three different Δm^2 values. The most sensitive analysis predicts, for a 20 kton \times year exposure, a total background of 4.4 events for a total τ selection efficiency of 33%.

ν NC rejection: Neutral current events contribute to the background from four sources: (1) electrons from Dalitz decays, (2) early photon conversions, (3) interacting charged pions and (4) π^\pm/π^0 overlap. Table V summarizes the rejection power of kinematics criteria for the four sources that contribute to ν NC background. The requirement on the electron candidate energy $E_e > 1$ GeV suppresses about one third of the Dalitz, pion overlap and π^0 conversions induced backgrounds, since electrons in the jet are soft.

The ultimate discrimination of these backgrounds relies primarily on the imaging capabilities and on dE/dx measurements. The combination of dE/dx information together with kinematics criteria is sufficient to reduce ν NC background to a negligible level.

ν_μ CC rejection: Charged current events can contribute to the background in a similar way as the neutral current events described above when the leading muon escapes detection. In case the muon is not identified, the event will appear in first instance as a neutral current event. The source of electrons which can induce backgrounds are then similar to those discussed previously and are reduced to a negligible level for reasons already discussed. A more important source of background specific to charged current interactions comes from the decays of charmed mesons. At the CNGS energies $\sigma(\nu_\mu N \rightarrow \mu c X)/\sigma(\nu_\mu N \rightarrow \mu X) \approx 4\%$, therefore for a total exposure of 20 kton \times year we expect to collect about 200 events where a charmed meson decays into a positron and a neutrino. These events resemble kinematically the real ν_τ events, since they have a neutrino in the final state and possess a softer energy spectrum and a genuine sizeable missing transverse momentum. After all cuts, the expected number of charm induced background events $n_{\text{CC (charm)}}^b$ for a total exposure of 20 kton \times year is at the level of 1 event.

5.5. Combined $\nu_\mu \rightarrow \nu_\tau$ sensitivity

Table VI summarizes the expectations for the $\tau \rightarrow e$ analysis once kinematics criteria and muon vetoes have been applied to every potential back-

ground source. In conclusion, we obtain for a 20 kton × year exposure, that the overall electron selection efficiency is 32% for an expected number of about five background events. The expected number of fully identified tau events at the central Δm^2 value of $3.5 \times 10^{-3} \text{ eV}^2$ is 35.

TABLE VI

$\tau \rightarrow e$ analysis summary. For a total exposure of 20 × year we show the expected number of τ events for different Δm^2 values. The last three columns show the expected background.

$\Delta m^2 \text{ (eV}^2\text{)}$	ν_τ CC	$\nu_e, \bar{\nu}_e$ CC	$\nu_\mu, \bar{\nu}_\mu$ CC	ν_μ NC
1×10^{-3}	3			
2×10^{-3}	12			
3×10^{-3}	26			
3.5×10^{-3}	35	4.1	1.0	< 1
5×10^{-3}	71			
7×10^{-3}	121			
1×10^{-2}	248			

Some increase in sensitivity can be achieved by including hadronic decays of the tau. These channels suffer however from low efficiency. The isolation method used to discriminate between signal and the main background coming from neutral current interaction has a strong energy dependence, making these channels rather insensitive to the low Δm^2 region. They can however be used efficiently for the upper part of the Δm^2 region.

The 90%C.L. exclusion curve for $\nu_\mu \rightarrow \nu_\tau$ oscillations is shown in figure 4 in case of negative result after four years of running at the CNGS (shared mode). The sensitivity is such as to cover completely the region indicated by the SuperKamiokande detector. It should be stressed that for most of the Δm^2 region allowed by SuperKamiokande, the rate of ν_τ CC events is so high as to give a statistical excess even prior or with mild kinematical cuts. See for example in Table IV, the number of ν_τ CC with $\tau \rightarrow e$ for the best fit value $\Delta m^2 = 3.5 \times 10^{-3} \text{ eV}^2$ is $\simeq 110$ events, while the background from $\nu_e, \bar{\nu}_e$ CC amounts to about 470 events. Such an excess will be visible (for example in the energy spectrum) even prior to kinematical cuts. The actual cuts will therefore be imposed *a posteriori* in order to optimize the sensitivity for a given Δm^2 .

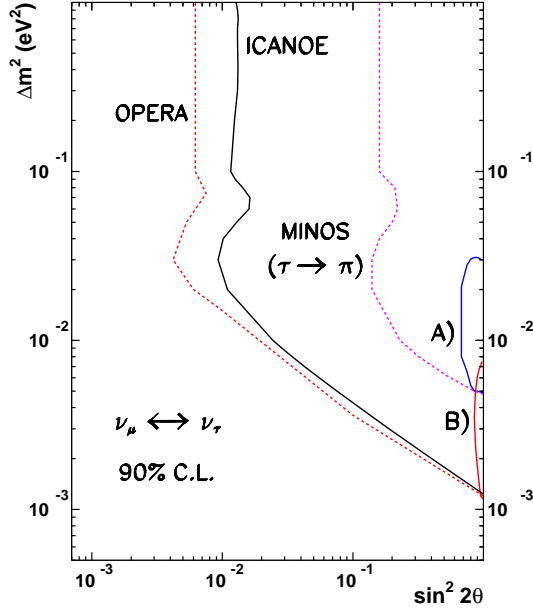


Fig. 4. Negative result excluded region for direct tau appearance search. The 90% C.L. for ICANOE with 10% and 5% systematic error, for MINOS with 1% systematic error and for OPERA (limited by statistics) are shown. The 90%, and 99% signal region of LSND is also shown. The exposure for ICANOE and OPERA is equivalent to four years at the CNGS. For MINOS, it corresponds to the PH2(high) beam.

5.6. Electron appearance

This search is motivated by the LSND claim but also to look for possible small ν_e mixing in the low Δm^2 region in a three neutrino mixing scenario. The search is rather simple: the events with leading electron are selected as for the $\tau \rightarrow e$ search. Non leading electrons are rejected by imaging. A simple event counting is performed for $E_{\text{vis}} < 20$ GeV. No energy shape information has been included so far. Since there is no “near” station planned at the CNGS, one has to rely on the prediction of the beam in absence of oscillations based on simulations. We anticipate that this will introduce a systematic error on the amount of ν_e CC events at the level of 5–10%. In case of negative result the confidence limits are shown in figure 5. These limits cover well the LSND region and can test mixing down to 10^{-3} for large Δm^2 and $\Delta m^2 = 4 \times 10^{-4}$ eV² for maximal mixing.

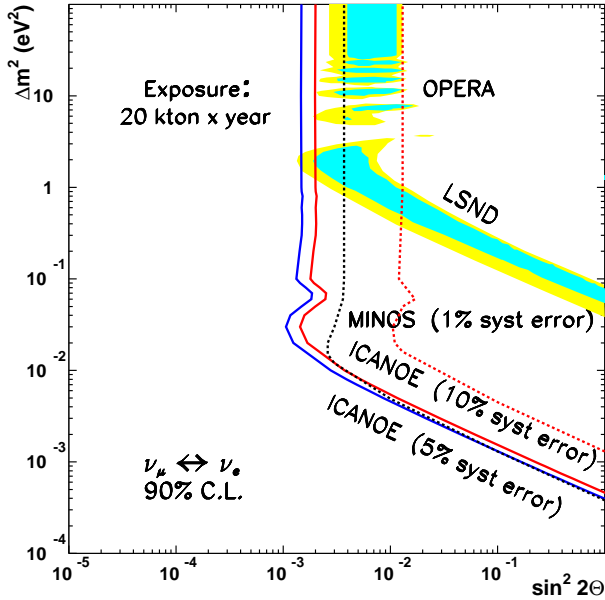


Fig. 5. Negative result excluded region for electron appearance search. The 90% C.L. for ICANOE with 10% and 5% systematic error, for MINOS with 1% systematic error and for OPERA (limited by statistics) are shown. The 90%, and 99% signal region of LSND is also shown. The exposure for ICANOE and OPERA is equivalent to four years at the CNGS. For MINOS, it corresponds to two years with the PH2 (high) beam.

5.7. Atmospheric neutrinos

The physics goals of the new atmospheric neutrino measurements are to firmly establish the evidence of neutrino oscillations with a different experimental technique, possibly free of systematic biases, measure the oscillation parameters and clarify the nature of the oscillation mechanism. ICANOE will provide, in addition to comfortable statistics, an observation of atmospheric neutrinos of a very high quality. Unlike measurements obtained up to now in Water Cherenkov detectors, which are in practice limited to the analysis of “single-ring” events, complicated final states with multi-pion products, occurring mostly at energies higher than a few GeV, will be completely analyzed and reconstructed in ICANOE. This will be a significant improvement with respect to previous observations.

We have considered the following three methods: (a) ν_μ disappearance: detection of the oscillation pattern in the L/E distribution, where L is the neutrino pathlength and E its energy; (b) ν_τ appearance: comparison of the NC/CC with expectation; (c) direct ν_τ appearance: comparison of upward

and downward rates of “tau-like” events together with the well established ones (d) the double ratio, $(\nu_\mu/\nu_e)_{\text{obs}}/(\nu_\mu/\nu_e)_{\text{MC}}$; (e) up/down asymmetry.

The tau appearance measurements can shed light on the nature of the oscillation mechanism, by discriminating between the hypothesis of oscillations into a sterile or a tau neutrino. The ν_τ appearance method is based on ν_τ CC interactions with ν_τ decaying into hadrons, hence to “neutral-current-like” events of high energy. An excess of “NC-like” events from the bottom will indicate the presence of oscillation to the ν_τ flavour. A kinematical analysis of the final state particles in the event can be used to further improve the statistical significance of the excess. Such a feature can only be obtained in a detector with the resolution of the ICANOE liquid target, in which all final state particles can be identified and precisely measured. The kinematical method would allow the evidence for “tau-like” events in the atmospheric neutrino beam.

Both the ν_μ disappearance and the direct ν_τ appearance methods are weakly depending on the predictions of neutrino event rates, since they rely on the comparison of rates induced by a downward going and upward going neutrinos.

The NC/CC method, already investigated by SuperKamiokande, can be significantly improved compared to this latter measurement. In ICANOE, imaging in the liquid target provides a clean bias free identification of neutral-current, independent on the hadronic final state, since the identification is based on the absence of an electron or a muon in the final state.

In the following sections, we will study our results for three different exposures: 5 kton \times year corresponding to 1 year of operation, 20 kton \times year for 4 years and an ultimate exposure of 50 kton \times year or 10 years of operation.

5.8. Event containment and muon measurement

The muon measurement is crucial to most atmospheric neutrino analyses. In ICANOE, we achieve the required performances using the multiple scattering measurement rather than resorting to a high-density, coarser resolution detector. Keeping a low density detector, high granularity detector imaging allows in addition the identification and measurement of electrons and individual hadrons in the event.

“Fully contained events” are those for which the visible products of the neutrino interaction are completely contained within the detector volume. “Partially contained events” are ν_μ CC events for which the muon exits the detector volume (only muons are penetrating enough).

Figure 6 shows containment of charged current events for different incoming neutrino energies or muon momentum thresholds. Clearly, because of the average energy loss of the muon in argon (about 210 MeV/m for a

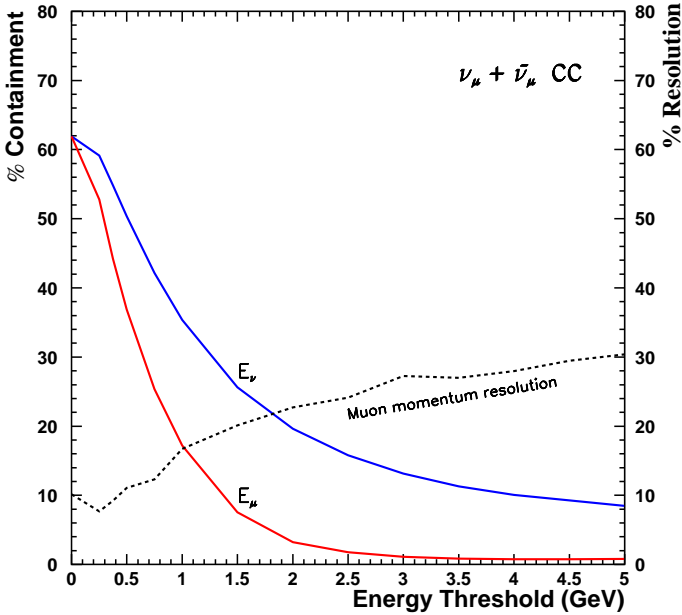


Fig. 6. Integral distributions showing the containment for ν_μ CC as a function of the neutrino energy and the leading muon momentum (solid lines). Differential distribution showing the muon momentum resolution as a function of muon momentum (dashed line), including both contained and partially contained events.

m.i.p.), muons produced in neutrino events are often energetic enough to escape from the subdetector volume.

It should first be noted that for contained events the muon energy resolution is 4% from dE/dx measurements. For escaping muons, the high granularity of the imaging allows to collect a very precise determination of the track trajectory. Therefore the multiple scattering method can be effectively used to estimate the momentum of the escaping muons. This method requires in practice tracks in excess of 1 meter and works extremely well in the relevant energy range of atmospheric neutrino events (typically below 10 GeV).

The average muon momentum resolution as a function of the energy threshold is shown in figure 6. This resolution has been computed using the range measurement for contained muons and multiple scattering method for the escaping ones. For energies below 1 GeV, the average muon momentum resolution is about 10%. It increases slowly as a function of the muon momentum and reaches about 30% at 5 GeV.

5.9. ν_μ disappearance — L/E studies

In order to verify that atmospheric neutrino disappearance is really due to neutrino oscillations, an effective method consists in observing the modulation given by the characteristic oscillation probability:

$$P\left(\frac{L}{E}\right) = 1 - \sin^2(2\theta) \sin^2\left(1.27\Delta m^2 \frac{L}{E}\right) \quad (1)$$

with L in km, E in GeV, Δm^2 in eV^2 . This modulation will be characteristic of a given Δm^2 , when the event rate is plotted as a function of the reconstructed L/E of the events when compared to theoretical predictions. The ratio of the observed and predicted spectra has the advantage of being quite insensitive to the precise knowledge of the atmospheric neutrino flux, since the oscillation pattern is found by dips in the L/E distribution while the neutrino interaction spectrum is known to be a slowly varying function of L/E . Such a method is in principle capable of measuring Δm^2 exploiting atmospheric neutrino events.

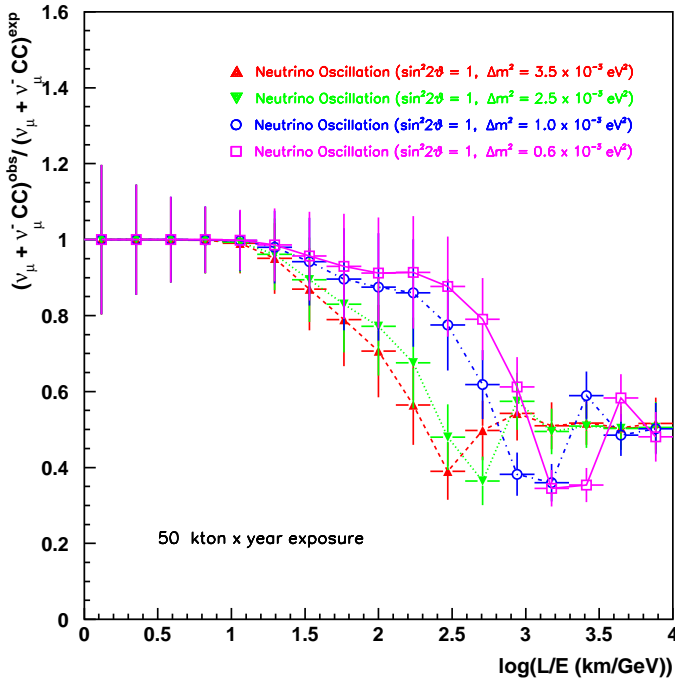


Fig. 7. Survival probability as a function of the L/E ratio assuming neutrino oscillation hypothesis and for various Δm^2 values and for 50 kton \times year. Only statistical error has been considered.

A smearing of the modulation is introduced by the finite L/E resolution of the detection method. Precise measurements of energy and direction of both the muon and hadrons are therefore needed in order to reconstruct precisely the neutrino L/E . This is quite well achieved in ICANOE. The contained muons can be measured with a resolution of 4%, while the non-contained muons are measured by multiple scattering method .

The RMS reconstructed L/E resolution is about 30% for events with $E_{\text{visible}} > 1$ GeV.

The ν_μ survival probability as a function of L/E let us determine the value of Δm^2 in case of oscillation is confirmed. In figure 7 we can see the survival probabilities of ν_μ for neutrino oscillation hypothesis and four different values of Δm^2 . The first minimum on the survival probability happens at highest L/E values for the lowest Δm^2 values, and allows us to discriminate between them for an exposure of 50 kton \times year.

5.10. (Direct) appearance of tau neutrinos

For $\Delta m^2 \leq 10^{-2}$ eV², oscillations of ν_μ into ν_τ would in fact result in an excess of “neutral-current-like” events produced by upward neutrinos with respect to downward, since charged-current ν_τ interactions would contribute to the “neutral-current-like” event sample, due to the large τ branching ratio into hadronic channels. Moreover, due to threshold effect on τ production, this excess would be important at high energy. Oscillations into a sterile neutrino would instead result in a depletion of upward muon-less events. Discrimination between $\nu_\mu \rightarrow \nu_\tau$ and $\nu_\mu \rightarrow \nu_s$ is thus obtained from a study of the asymmetry of upward to downward muon-less events. Because this method works with the high energy component of atmospheric neutrinos, it becomes effective for relatively large values of Δm^2 ($\geq 3 \times 10^{-3}$ eV²).

TABLE VII

Expected $\nu_\tau, \bar{\nu}_\tau$ absolute rates for five different Δm^2 with FLUKA-3D fluxes and relative to FLUKA-1D and Bartol fluxes.

Δm^2 (eV ²)	$\nu_\tau + \bar{\nu}_\tau$ CC (NUX, Fluka 3D flux)			Rel. to Fluka 1D	Rel. to Bartol
	Rate (kton \times year)				
	DIS	QE	Sum		
5×10^{-4}	0.11	0.11	0.22	0.96	0.81
1×10^{-3}	0.28	0.18	0.46	1.02	0.84
3.5×10^{-3}	0.59	0.21	0.80	1.00	0.81
5×10^{-3}	0.64	0.24	0.88	1.01	0.80
1×10^{-2}	0.70	0.20	0.90	0.99	0.78

Charged current ν_τ rates for five Δm^2 hypothesis: 5×10^{-4} , 1×10^{-3} , $3.5 \times 10^{-3} \text{eV}^2$, $5 \times 10^{-3} \text{eV}^2$ and $1 \times 10^{-2} \text{eV}^2$ are listed in Table VII. We see that the rates saturate at about one event per kton \times year for the larger Δm^2 values. Such small rates pose a major experimental challenge in the detection of ν_τ in the cosmic ray induced neutrino flux.

The total visible energy (E_{visible}) is a suitable discriminant variable to enhance the S/B ratio. After cuts, surviving events are classified as: n_b (number of expected downward going background) and $n_t = n_b + n_s$ (number of expected upward going events, where n_s is the number of taus). The statistical significance of the expected n_s excess is evaluated following two procedures:

- The f_b and f_t pdf's are integrated over the whole spectrum of possible measured r values and the overlap between the two is computed:

$$P_\alpha \equiv \int_0^\infty \min(f_b(r), f_t(r)) dr,$$

where f_b and f_t are the Poisson p.d.f.'s for means $\mu = n_b$ and $\mu = n_t$ respectively. The smaller the overlap integrated probability (P_α) the larger the significance of the expected excess.

- Computing the probability

$$P_\beta \equiv \int_{n_t}^\infty \frac{e^{-n_b} n_b^r}{r!} dr$$

that, due to a statistical fluctuation of the unoscillated data, we measure n_t events or more when n_b are expected.

For a 50 kton \times year exposure, the results of a search based on E_{visible} are shown in Table VIII. We see that a cut on visible energy between 6 and 7 GeV results in: (1) an overlap integrated probability between the two distributions amounting to 25–26%. (2) a Poisson probability that the measured excess (“ τ bottom”) corresponds to a statistical fluctuation is 0.6–0.8%.

The search for ν_τ appearance can be improved taking advantage of the special characteristics of ν_τ CC and the subsequent decay of the produced τ lepton when compared to CC and NC interactions of ν_μ and ν_e , *i.e.* by making use of \vec{P}_{lepton} and \vec{P}_{hadron} .

The information related to the directionality of the incoming neutrino (*i.e.* the beam direction!) is missing. As a result, we have three kinematical

TABLE VIII

Number of NC and tau events as a function of the visible energy cut. The statistical sample used corresponds to an exposure of 50 kton \times year.

50 kton \times year exposure				
E_{visible} cut	ν NC top	τ bottom	P_α (%)	P_β (%)
> 1 GeV	327	22	55.0	10.8
> 2 GeV	150	22	38.6	3.54
> 3 GeV	95	21	30.6	1.6
> 4 GeV	67	20	25.3	0.8
> 5 GeV	51	17	27.3	0.9
> 6 GeV	40	16	24.6	0.6
> 7 GeV	33	14	26.6	0.8
> 8 GeV	28	13	26.7	0.8
> 9 GeV	23	12	26.2	0.7
> 10 GeV	21	11	28.3	0.9

independent variables in order to separate signal from background. After a careful evaluation of the performance of different combinations of variables, we decided to use: E_{visible} , y_{bj} (the ratio between the total hadronic energy and E_{visible}), and Q_T (the transverse momentum of the τ candidate with respect to the total measured momentum) which contains the information on the isolation of the tau candidate from the recoiling jet.

The chosen variables are not independent one from another but show correlations between them. These correlations can be exploited to reduce the background. In order to maximize the separation between signal and background, we use three dimensional likelihood functions $\mathcal{L}(Q_T, E_{\text{visible}}, y_{bj})$ where correlations are taken into account. The best sensitivity is achieved for the following set of cuts: $\ln \lambda_\pi > 3$, $\ln \lambda_\rho > 0.5$ and $\ln \lambda_{3\pi} > 0$. The expected number of NC background events amounts to 12 (top) while 12+11 = 23 (bottom) are expected. This corresponds to a P_α of 18.3%. In the case we consider E_{visible} as the unique discriminating variable, a similar number of background events is obtained demanding $E_{\text{visible}} > 14$ GeV. With this cut, the expected number of τ events is 7 and the P_α is 37%. Therefore, for the same level of background, the approach using the ratio of three dimensional likelihood functions enhances the number of expected signal events by approximately 50%.

Finally, in figure 8 we present the Poisson probability P_β for the measured excess of upward going events to be due to a statistical fluctuation as a function of the exposure. The bottom curve corresponds to the case where no kinematical selection has been applied and only a cut on $E_{\text{visible}} > 6$ GeV

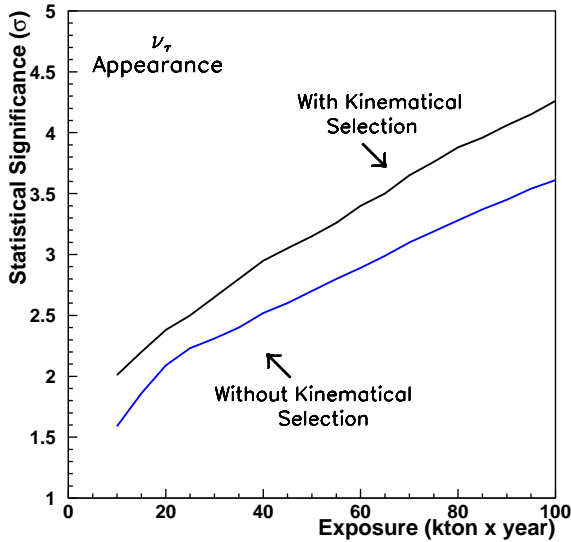


Fig. 8. Probability for the measured excess of upward going events to be due to a statistical fluctuation of the data as a function of the exposure.

is used. We see that for exposures around 30 kton \times year, in case we use the kinematical selection algorithm, the observed excess corresponds to a 2.6 σ effect. This effect is larger than 3 σ for an exposure of 50 kton \times year.

5.11. Determination of the oscillation matrix

In the most general case, the 3 \times 3 unitary mixing can be parametrized in analogy to the quark sector

$$U = \begin{pmatrix} c_{12}c_{13} & s_{12}c_{13} & s_{13}e^{-i\delta} \\ -s_{12}c_{23} - c_{12}s_{13}s_{23}e^{i\delta} & c_{12}c_{23} - s_{12}s_{13}s_{23}e^{i\delta} & c_{13}s_{23} \\ s_{12}s_{23} - c_{12}s_{13}c_{23}e^{i\delta} & -c_{12}s_{23} - s_{12}s_{13}c_{23}e^{i\delta} & c_{13}c_{23} \end{pmatrix}, \quad (2)$$

where $s_{ij} = \sin \theta_{ij}$, $c_{ij} = \cos \theta_{ij}$.

In the one mass scale approximation, the oscillation phenomena will be determined by the three parameters Δm_{32}^2 , θ_{23} and θ_{13} . These parameters can be determined by combining the appearance and disappearance signatures together with atmospheric measurements.

We report on fits performed using the data that ICANOE could collect in four years of running. We combine the information coming from CNGS appearance and disappearance data and atmospheric analyses: $\chi^2 = \chi_{\text{CNGS}-e}^2 + \chi_{\text{CNGS}-\mu}^2 + \chi_{\text{atm}}^2$. Large but conservative systematic errors have

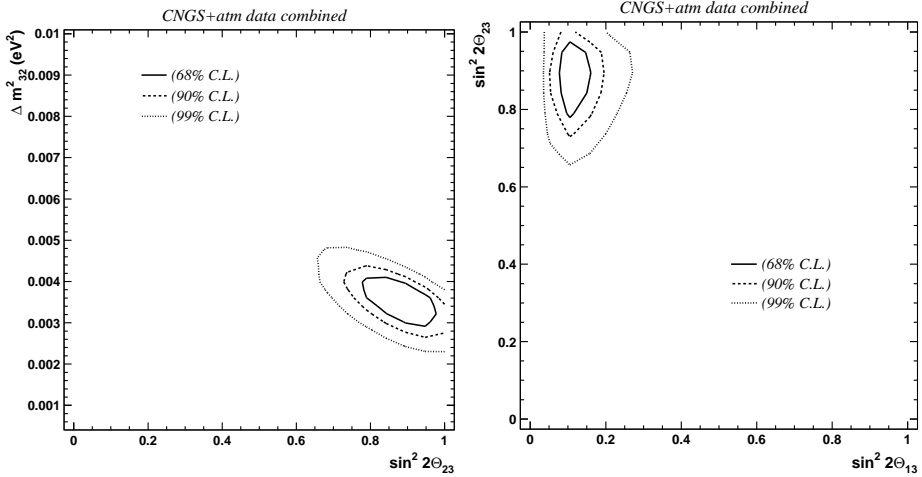


Fig. 9. Determination of the parameters Δm_{32}^2 , $\sin^2 2\theta_{23}$ (left) and $\sin^2 2\theta_{23}$ and $\sin^2 2\theta_{13}$ (right), using the CNGS electron appearance and disappearance data combined with atmospheric data (right). For each plot, the χ^2 value of the fit is plotted as a function of two parameters. When computing the χ^2 for two parameters, the third one is left free. The 68%, 90% and 99% corresponds to respectively $\chi^2 + 2.4$, $+4.6$, and $+9.2$ regions.

been included: muon spectrum uncorrelated bin-to-bin $\pm 30\%$, electron spectrum uncorrelated bin-to-bin $\pm 10\%$, tau spectrum uncorrelated bin-to-bin $\pm 10\%$, Zenith angle distributions $\pm 20\%$.

The improvement of the determination of the oscillation parameters obtained by the combination of the different observables is easily understandable. The atmospheric data alone imposed a constraint on $\sin^2 2\theta_{23}$ which, when combined with the CNGS electron appearance data drastically improves the precision in the measurement of Δm_{32}^2 . Moreover, the capability to discriminate ν_e 's from ν_τ 's allows an accurate determination of the mixing angle θ_{13} as well.

For example, for given reference parameters, and for a total exposure of 20 kton \times year for beam neutrinos and 25 kton \times year for atmospheric neutrinos, ICANOE would measure the parameters governing the oscillation with the following precisions:

$$\begin{aligned}\Delta m_{32}^2 &= (3.5 \pm 0.4) \times 10^{-3} \text{ eV}^2, \\ \sin^2 2\theta_{23} &= 0.90 \pm 0.12, \\ \sin^2 2\theta_{13} &= 0.10 \pm 0.04.\end{aligned}\tag{3}$$

The quantitative results can be observed in figure 9 (left, Δm_{32}^2 versus $\sin^2 2\theta_{23}$; right, $\sin^2 2\theta_{23}$ versus $\sin^2 2\theta_{13}$) where the allowed parameter

regions at the 68%, 90% and 99% C.L. are drawn. We observe that by combining all the available data sets, the region of allowed values is reduced to a small closed region of the parameter space.

6. Conclusion

The ν_μ disappearance has been seen in atmospheric neutrino experiments. This has led to the “evidence for neutrino oscillations”.

The main problem in neutrino physics is to perform the right experiment(s) to *elucidate in a comprehensive way the pattern of neutrino masses and mixings*.

The long baseline experiments will play a fundamental role at settling definitively the question of flavor oscillation and at measuring with good precision the full mixing matrix.

Solving the most intriguing neutrino oscillation phenomenology will definitely represent a fundamental milestone in particle physics.

I thank the organizers of the Epiphany conference, and especially Prof. M. Jeżabek, for the excellent organization and the level of the stimulating conference. The help of A. Bueno, M. Campanelli, A. Ferrari and J. Rico is greatly acknowledged.

REFERENCES

- [1] K.S. Hirata *et al.* [KAMIOKANDE-II Collaboration], *Phys. Lett.* **B205**, 416 (1988).
- [2] Y. Fukuda *et al.* [SuperKamiokande Collaboration], *Phys. Rev. Lett.* **81**, 1562 (1998), [hep-ex/9807003](#).
- [3] W.W. Allison *et al.* [Soudan-2 Collaboration], *Phys. Lett.* **B449**, 137 (1999), [hep-ex/9901024](#).
- [4] F. Ronga *et al.* [MACRO Collaboration], Neutrino Oscillations at High Energy by MACRO, [hep-ex/9905025](#). The MACRO Coll., M. Ambrosio *et al.*, *Phys. Lett.* **B434**, 451 (1998), [hep-ex/9807005](#).
- [5] A. Para, *Acta Phys. Pol.* **B31**, 1313 (2000).
- [6] G. Acquistapace *et al.*, CERN 98-02 and INFN/AE-98/05; R. Bailey *et al.*, CERN-SL/99-034(DI) and INFN/AE-99/05.
- [7] D. Kielczewska, *Acta Phys. Pol.* **B31**, 1181 (2000).
- [8] ICARUS and NOE Collaborations, ICANOE — a Proposal for a CERN–GS Long Baseline and Atmospheric Neutrino Oscillation Experiment, LNGS P21/99, CERN/SPSC 99-25, SPSC/P314. Updated information is available at <http://pcnometh4.cern.ch>.

- [9] ICARUS Collaboration, Laboratori Nazionali del Gran Sasso (LNGS) Int. Note, LNGS-94/99 (Vols I–II), unpublished; LNGS-95/10, unpublished. P. Benetti *et al.*, *Nucl. Instrum. Methods* **A327**, 173 (1993); *Nucl. Instrum. Methods* **A332**, 395 (1993); P. Cennini *et al.*, *Nucl. Instrum. Methods* **A333**, 567 (1993); *Nucl. Instrum. Methods* **A345**, 230 (1994); *Nucl. Instrum. Methods* **A355**, 660 (1995).
- [10] The ICARUS collaboration, ICARUS-Like Technology for Long Baseline Neutrino Oscillations, CERN/SPSC/98-33 & M620, 1998.
- [11] ICARUS–CERN–Milano Coll., CERN/SPSLC 96-58, SPSLC/P 304, December 1996; J.P. Revol *et al.*, ICARUS-TM-97/01, 5 March 1997, unpublished.
- [12] S. Katsanevas, *Acta Phys. Pol.* **B31**, 0000 (2000).
- [13] F. Arneodo *et al.* [ICARUS Collaboration], The ICARUS 50 l LAr TPC in the CERN Neutrino Beam, [hep-ex/9812006](#).
- [14] A. Bueno, M. Campanelli, A. Ferrari, A. Rubbia, Nucleon Decay studies in a large Liquid Argon detector, to be published in International Workshop on Next Generation Nucleon Decay and Neutrino Detector (NNN 99), Stony Brook, New York, 23–25 Sep. 1999.